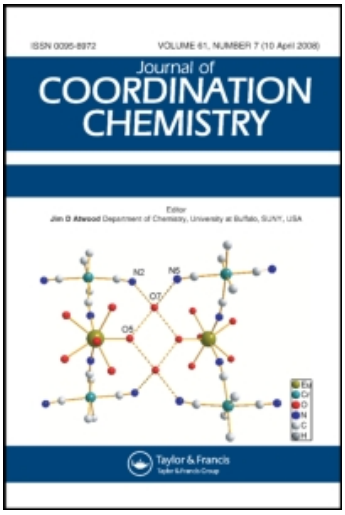

**Journal of Coordination Chemistry**
Publication details, including instructions for authors and subscription information:
http://www.informaworld.com/smpp/title~content=t713455674

# Cu(II) AND Ni(II) COMPLEXES OF *N, N'-bis*(2-AMINOETHYL)-OXAMIDE AND *N, N'-bis*(3-AMINOPROPYL) OXAMIDE: A POTENTIOMETRIC AND SPECTROPHOTOMETRIC STUDY

Sieglinde Cattoir[a]; Gerrit G. Herman[a]; André M. Goeminne[a]; Herman O. Desseyn[b]
[a] Laboratorium voor Algemene en Anorganische Chemie, Universiteit Gent, Gent, Belgium [b] Laboratorium voor Anorganische Chemie, Universiteit Antwerpen (RUCA), Antwerpen, Belgium

**To cite this Article** Cattoir, Sieglinde , Herman, Gerrit G. , Goeminne, André M. and Desseyn, Herman O.(1996) 'Cu(II) AND Ni(II) COMPLEXES OF *N, N'-bis*(2-AMINOETHYL)-OXAMIDE AND *N, N'-bis*(3-AMINOPROPYL) OXAMIDE: A POTENTIOMETRIC AND SPECTROPHOTOMETRIC STUDY', Journal of Coordination Chemistry, 38: 3, 245 — 258
**To link to this Article: DOI:** 10.1080/00958979608022710
**URL:** http://dx.doi.org/10.1080/00958979608022710

*J. Coord. Chem.*, 1996, Vol 38, pp. 245–258
Reprints available directly from the publisher
Photocopying permitted by license only



# Cu(II) AND Ni(II) COMPLEXES OF *N, N'-bis*(2-AMINOETHYL)-OXAMIDE AND *N, N'-bis*(3-AMINOPROPYL) OXAMIDE: A POTENTIOMETRIC AND SPECTROPHOTOMETRIC STUDY

SIEGLINDE CATTOIR, GERRIT G. HERMAN,* ANDRÉ M. GOEMINNE

*Laboratorium voor Algemene en Anorganische Chemie, Universiteit Gent, Krijgslaan 281 S3, 9000 Gent, Belgium*

and HERMAN O. DESSEYN

*Laboratorium voor Anorganische Chemie, Universiteit Antwerpen (RUCA), Groenenborgerlaan 171, 2020 Antwerpen, Belgium*

*(Received July 12, 1995)*



Extensive potentiometric and spectrophotometric (visible region) data resulted in the unravelling of the complete details of complex formation of *N,N'-bis*(2-aminoethyl) oxamide ($L^1$)and *N,N'-bis*(3-aminopropyl) oxamide ($L^2$). This study reveals both similarities and differences in complex formation for these ligands. Earlier reports gave evidence for the formation of a $Cu_3L_2H_{-4}$ complex of $L^2$. We show that $L^1$ forms a $Cu_2L_2H_2$ complex. This difference in behaviour is due to a decrease in stability of the $CuLH_{-2}$ complex of $L^2$ compared to that of $L^1$. The complexation of $Ni^{2+}$ by $L^1$ is also discussed.

KEYWORDS: aminoalkyloxamides, stability constants, copper, nickel, potentiometry, spectrophotometry.

## INTRODUCTION

The coordinating properties of the amide group in general and of the oxamide group in particular have been the subject of two reviews. Sigel and Martin[1] discussed a wide range of amides, in both solid state and in solution. Ojima and Nonoyama focused on magnetic properties and spectroscopic data.[2]

We have studied $Cu^{2+}$ and $Ni^{2+}$ complexes of a range of aminoalkyl substituted oxamides. Griesser and Fallab have studied $Cu^{2+}$ complexes of *N,N'-bis*(2-aminoethyl) oxamide ($L^1$) (see Figure 1 for chemical structure) in water.[3] They found the following complexes: CuL, $Cu_2LH_{-2}$, $CuLH_{-1}$, $CuLH_{-2}$, $Cu_2LH_{-3}$ and $Cu_2LH_{-4}$. The last two complexes are only formed under conditions in which the

* Author for correspondence.

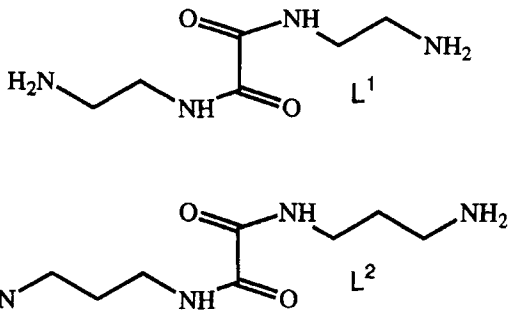


**Figure 1** Structural representation of *N,N'-bis*(2-aminoethyl) oxamide ($L^1$) and *N,N'-bis*(3-aminopropyl) oxamide ($L^2$).

molar ratio $Cu^{2+}$: $L^1$ exceeds 2:1. Lloret *et al.* studied amino alkyl substituted oxamides including $Cu^{2+}$ complexes of *N,N'-bis* (3-aminopropyl) oxamide ($L^2$) (see Figure 1 for chemical structure).[4,5,6,7] They found that $L^2$ and $Cu^{2+}$ form the following complexes: $Cu_2LH_{-2}$, $CuLH_{-2}$, $Cu_3L_2H_{-4}$ and $Cu_4L_3H_{-6}$.

However, analysis of preliminary data clearly showed that to some extent we could not fully support the complex models suggested in these reports. In order to formulate an improved model for the complexation of these ligands, and to re-evaluate our initial findings, we carried out a large number of potentiometric titrations and completed our data with an electronic spectroscopy study. In addition, complex formation of $L^1$ with $Ni^{2+}$ was also examined.



## EXPERIMENTAL

### *Reagents*

All chemicals were of analytical grade, and used as received unless specifically noted and obtained from the following sources: $Ni(NO_3)_2.6H_2O$, $Cu(NO_3)_2.3H_2O$, $KNO_3$, 1,2-diaminoethane, 1,3-diaminopropane, KOH and HCl (Acros Chimica), diethyloxalate, methanol, ethanol (Merck).

### *Solutions*

Distilled and deionised water (Milli-Q quality, conductance <0.05 μS $cm^{-1}$) was used for all solutions. Carbonate-free (<0.5%) potassium hydroxide solutions (*ca* 0.200 mol $dm^{-3}$) were prepared from Titrisol ampoules and were standardised by titration with HCl. HCl was standardised by argentometry. Metal ion stock solutions were prepared from metal nitrates and were standardised by titration with the disodium salt of ethylenediaminetetraacetic acid (edta) in the presence of a small amount of the Hg(edta) complex, using appropriate conditions and electrodes (mercury and calomel electrode).[8] All final solutions for potentiometric and spectrometric titrations were made up to an ionic strength of 0.1 mol $dm^{-3}$ with potassium nitrate.

*Synthesis of $L^1$ and $L^2$*

$L^1$ was obtained by slowly adding diethyl oxalate (1.0 mol) to 1,2-diaminoethane (20.0 mol) at room temperature. $L^2$ was obtained in a similar way, using 1,3-diaminopropane instead of 1,2-diaminoethane. The solution was filtered and the excess amine was distilled off under reduced pressure. The residue was dissolved in methanol and recrystallised from methanol/ether (yield 80%). The CI mass spectrum (Riber 10–10B) (Nermag S.A.) quadrupole mass spectrometer showed *m/z* to be 175 ($M^+$) (calc. 175) for $L^1$ and 203 (calc. 203) for $L^2$. The IR spectrum of $L^1$ (Bruker IFS 113v Fourier transform spectrometer) shows ν(NH) at 3295 $cm^{-1}$, amide I (ν(CO)) at 1649 $cm^{-1}$ and amide II (δ(NH)[ + ν(CN)]) and III (ν(CM)[ + δ[NH)]) at 1528 $cm^{-1}$ and 1231 $cm^{-1}$, respectively. The IR spectrum of $L^2$ shows ν(NH) at 3295 $cm^{-1}$, amide I at 1649 $cm^{-1}$ and amide II and III at 1528 $cm^{-1}$ and 1231 $cm^{-1}$, respectively.

*Synthesis of the hydrochlorides of $L^1$ and $L^2$*

To a concentrated solution of $L^1$ or $L^2$ in ethanol was slowly added 12 mol $dm^{-3}$ HCl to pH 1. The precipitate was recrystallised from 70% ethanol/water (yield 65%). The purity of the salts, obtained by argentometry and KOH-potentiometry was 99.5%.



*Potentiometric measurements*

Potentiometric measurements were carried out using a titration system equipped with a Schott CG841 pH-meter and a Schott T200 burette (total volume 5 $cm^3$ or 10 $cm^3$). The pH meter was fitted with a Schott glass electrode and a Schott Ag/AgCl reference electrode with a second salt bridge filled with 0.1 mol $dm^{-3}$ $KNO_3$ solution. A Schott titration assembly was used with a thermostatted vessel (50 $cm^3$ or 80 $cm^3$) and a magnetic stirrer. All titrations were performed at 25 ± 0.05°C under an atmosphere of nitrogen, presaturated with water vapour by bubbling through a 0.1 mol $dm^{-3}$ $KNO_3$ solution. The program TITRATE, slightly modified, was used to monitor the titration.[9]

The electrode system was calibrated as a hydrogen ion concentration probe (pH = $-\log[H^+]$) by titrations of hydrochloric acid (50 $cm^3$ of 0.00941 mol $dm^{-3}$ with standard potassium hydroxide titrant solution (*ca* 0.200 mol $dm^{-3}$). The concentration of HCl was determined by argentometry. The titration data were processed using Gran's method in order to calculate the standard cell potential (E°), the dissociation constant of water ($K_w$), together with the correction terms for changes in the liquid junction potential in strong acid medium, aj ($-\log[H^+] < 2.5$) and for non-linear electrode response in strong alkaline medium, bj ($-\log[H^+] > 11.5$).[10] The $pK_w$ value was found to be 13.78 in accord with literature values, aj = 420 mV $dm^3$ $mol^{-1}$ and bj = −90 mV $dm^3$ $mol^{-1}$.[11] The e.m.f. readings were converted into pH values using equation (*1*); pH values were obtained by successive approximations taking $[H^+]$ as zero at the start.

$$pH = (E^\circ - E + aj[H^+] + bjK_w[H^+]^{-1})/S \qquad (1)$$

The value for the Nernst slope, S, was obtained as the slope of the plot $pH_{calc}$ *versus* $E_{measured}$ for $2.5 < pH_{calc} < 4.5$ and $8.0 < pH_{calc} < 11.5$, and was found to be 59.0 ± 0.05 mV. The calibration parameters remained fairly constant with time.

All initial concentrations of $Cu^{2+}$, $Ni^{2+}$, ligand and HCl are given in Table I. This Table also includes the concentration of the base and the total number of pH values recorded in the titrations.

*Formation curves*

In order to test complex formation of $Ni^{2+}$ and $L^1$, formation curves were necessary. Equations (*2*) and (*3*) can be derived from mass-balances, on the condition that only complexes of the general form $M_p(LH_s)_t$ are formed. In this case the formation curve is obtained by plotting $\bar{n}$ *versus* $p(LH_s)$. The complexation of $Ni^{2+}$ by $L^1$ involves complexes of the general form $M_p(LH_{-1})_t$. An additional difficulty therefore is that the first amide deprotonation constant of the oxamide group is not known. This problem is by-passed by plotting $\bar{n}$ *versus* pL-pH instead of $\bar{n}$ *versus* $pLH_{-1}$. Consequently, this formation curve is shifted by $pK_{-1}$ to the actual formation curve. [L] and $\bar{n}$ for the formation of $M_p(LH_s)_t$, with $LH_u$ being the fully protonated ligand are given below.

$$[L] = \frac{(u - s)C_L - C_{OH} + [OH] - [H]}{\sum_{i=0}^{u-s-1} (u - s - i)\beta_{u-i}[H]^{u-i}} \qquad (2)$$

$$\bar{n} = \frac{C_L - [L]\sum_{i=0}^{u} \beta_i[H]^i}{C_M} \qquad (3)$$

*Electronic spectrophotometric measurements*

The electronic absorption spectra were recorded at 25°C on a Hewlett-Packard 8451A diode array spectrophotometer in the wavelength region of 190 nm to 820 nm. Consecutive spectra for systems involving rapid equilibria were obtained from titrations in a way similar to the potentiometric experiments; at each titration point a small amount of the titration solution was injected in a measuring cell of appropriate cell length and re-injected into the titration vessel after recording the spectrum. For systems involving slow equilibria, spectra were obtained from separate solutions for each titration point after an appropriate equilibration period. Experimental conditions are given in Table I.

*Calculation of equilibrium constants*

The overall stability constants $\beta_{pqr}$( = $[M_pL_qH_r]/[M]^p[L]^q[H]^r$) of the various species formed in aqueous solution were obtained from numerical analysis of all experimental e.m.f. data from the potentiometric titrations using SUPERQUAD.[12,13] Titration data obtained at different ligand to metal ratios and/or different initial concentrations of both ligand and metal were processed by SUPERQUAD as a

**Table I** Potentiometric and Spectrophotometric Titrations for $Cu^{2+}$ and $Ni^{2+}$ complexation of $L^1$ and $L^2$ at 25°C and I = 0,1 mol $dm^{-3}$ ($KNO_3$).

| n° titration | M/L | mmol M[a] | mmol L[b] | mmol H[c] | initial volume | $C_{OH}$[d] (mol $dm^{-3}$) | number of pts.[e] |
|---|---|---|---|---|---|---|---|
| $L^1$, Potentiometric Titrations | | | | | | | |
| 1 | | | 0.2551 | 0.6897 | 50 | 0.2217 | 108 |
| 2 | | | 0.1349 | 0.3467 | 15 | 0.2088 | 72 |
| 3 | | | 0.3958 | 0.9994 | 40 | 0.1960 | 90 |
| $L^2$, Potentiometric Titrations | | | | | | | |
| 4 | | | 0.3939 | 0.9956 | 40 | 0.1960 | 90 |
| 5 | | | 0.2515 | 0.6998 | 50 | 0.2217 | 90 |
| 6 | | | 0.3950 | 0.9587 | 80 | 0.2151 | 74 |
| $Cu^{2+}$ + $L^1$, Potentiometric Titrations | | | | | | | |
| 7 | 1/1 | 0.05355 | 0.04901 | 0.1240 | 80 | 0.2148 | 83 |
| 8 | 1/1 | 0.1071 | 0.09802 | 0.2480 | 80 | 0.2148 | 84 |
| 9 | 1/1 | 0.2142 | 0.1960 | 0.4960 | 80 | 0.2148 | 102 |
| 10 | 1/1 | 0.4284 | 0.3921 | 0.9919 | 80 | 0.2148 | 107 |
| 11 | 1/2 | 0.1071 | 0.2001 | 0.4834 | 80 | 0.2148 | 99 |
| 12 | 1/2 | 0.2142 | 0.4002 | 0.9668 | 80 | 0.2148 | 106 |
| 13 | 2/1 | 0.1885 | 0.0968 | 0.2877 | 50 | 0.1938 | 14 |
| 14 | 3/2 | 0.1885 | 0.1255 | 0.3446 | 50 | 0.2217 | 126 |
| 15 | 3/2 | 0.5355 | 0.3598 | - 0.0421 | 50 | 0.2088 | 100 |
| 16 | 3/2 | 0.05355 | 0.03598 | - 0.0042 | 50 | 0.2088 | 201 |
| 17 | 4/3 | 0.1696 | 0.1255 | 0.3446 | 50 | 0.2217 | 125 |
| $Cu^{2+}$ + $L^2$, Potentiometric Titrations | | | | | | | |
| 18 | 1/1 | 0.2056 | 0.1979 | 0.4790 | 80 | 0.2161 | 66 |
| 19 | 1/1 | 0.4112 | 0.3958 | 0.9580 | 80 | 0.2161 | 79 |
| 20 | 1/2 | 0.1028 | 0.1979 | 0.4790 | 80 | 0.2161 | 82 |
| 21 | 2/1 | 0.1885 | 0.0980 | 0.2901 | 50 | 0.1938 | 70 |
| 22 | 2/1 | 0.2639 | 0.1323 | 0.3493 | 50 | 0.1938 | 67 |
| 23 | 3/2 | 0.1885 | 0.1260 | 0.3500 | 50 | 0.2217 | 117 |
| 24 | 4/3 | 0.1697 | - 0.1260 | 0.3500 | 50 | 0.2217 | 115 |
| $Cu^{2+}$ + $L^1$, Spectrophotometric Titrations (cellength = 1 cm) | | | | | | | |
| 25 | 1/1 | 0.8575 | 0.8575 | 1.715 | 50 | 1.075 | 30 |
| 26 | 1/1 | 0.3430 | 0.3430 | 0.6860 | 50 | 1.075 | 31 |
| 27 | 2/1 | 0.6860 | 0.3430 | 0.6860 | 50 | 1.075 | 16 |
| $Cu^{2+}$ + $L^2$, Spectrophotometric Titrations (cellength = 1 cm) | | | | | | | |
| 28 | 1/2 | 0.4288 | 0.8575 | 1.715 | 52 | 1.075 | 11 |
| 29 | 1/1 | 0.8575 | 0.8575 | 1.029 | 70 | 1.075 | 31 |
| 30 | 2/1 | 1.029 | 0.5145 | 1.715 | 50 | 1.075 | 16 |
| $Ni^{2+}$ + $L^1$, Potentiometric Titrations | | | | | | | |
| 31 | 1/1 | 0.1997 | 0.2007 | 0.4846 | 80 | 0.1957 | 48 |
| 32 | 1/1 | 0.3994 | 0.4014 | 0.9692 | 80 | 0.1957 | 80 |
| 33 | 1/1 | 0.2995 | 0.3011 | 0.7269 | 80 | 0.1957 | 75 |
| 34 | 1/1 | 0.2995 | 0.3011 | 0.7269 | 80 | 0.1957 | 64 |
| 35 | 1/2 | 0.1040 | 0.1997 | 0.4826 | 80 | 0.2166 | 60 |
| 36 | 1/2 | 0.2080 | 0.3994 | 0.9652 | 80 | 0.2166 | 82 |
| 37 | 2/1 | 0.2080 | 0.09885 | 0.2413 | 50 | 0.2166 | 26 |
| $Ni^{2+}$ + $L^1$, Spectrophotometric Titrations (cellength 5, 2 or 1 cm)[f] | | | | | | | |
| 38 | 1/1 | 0.07987 | 0.08424 | 0.2017 | 20 | 0.2017 | 16 |
| 39 | 1/1 | 0.03195 | 0.03195 | 0.07720 | 16 | 0.1679 | 11 |
| 40 | 2/1 | 0.05200 | 0.02564 | 0.01299 | 5 | 0.2148 | 10 |

[a] mmol M = number of millimoles metal in initial solution. [b] mmol L = number of millimoles ligand in initial solution. [c] mmol H = number of milimoles HCl in initial solution. [d] $C_{OH}$ = concentration KOH (burette). [e] Number of pts. = the total number of pH values registered in the titration. [f] Pathlength is varied during the titrations in order to obtain optimal resolution.

single set of data and all chemically acceptable complexation models were tested. The best complexation model was selected on the basis of the statistics given by the program (overall σ-value, goodness of fit ($\chi^2$), standard deviation on the overall formation constants).[14] The program EQUIL was used to calculate simulated titration curves for a given model and stability constants.[15]

## RESULTS AND DISCUSSION

### *Protonation constants*

For the calculation of the protonation constants of $L^1$ and $L^2$, three KOH titrations per ligand were used. For each of the ligands 90 points were used in the minimizations. SUPERQUAD calculated σ-values of 2.8 ($L^1$) and 2.2 ($L^2$). The protonation constants are given in Table II.

### *$Cu^{2+}$ complexes*

Table I shows all solution data for the potentiometric titrations. All titrations in which the ratio total $Cu^{2+}$: total $L^1$ equals 1:1 are depicted in Figure 2. Titrations with varying metal: ligand ratio for both ligands are shown in Figures 3 and 4. All titrations show two distinct buffer regions.

### *$Cu^{2+}$ complexes; first buffer region*

The first buffer region in the 1:1 titrations is formed between a = 0 and a = 2 (a being the number of moles base added to the total number of moles ligand).

**Table II** Overall protonation contants ($\log K_i^H$) of $L^1$ and $L^2$ and overall stability constants ($\log\beta MpLqHr$) for $Cu^{2+}$ and $Ni^{2+}$ complexes of $L^1$ and $L^2$ (25°C I = 0.10 mol $dm^{-3}$ $KNO_3$); $\lambda_{max}$ and $\varepsilon_{max}$ values.

| | pqr code | Equilibrium Quotient(log units)[b] | $\lambda$max (nm) | $^{e}$max ($M^{-1}cm^{-1}$) |
|---|---|---|---|---|
| $[L^1H^+]/[L^1][H]$[a] | 011 | 9.229(3) | | |
| $[L^1H_2]/[L^1H][H]$ | 012 | 8.423(2) | | |
| $[L^2H]/[L^2][H]$ | 011 | 10.140(3) | | |
| $[L^2H_2]/[L^2H][H]$ | 012 | 9.381(3) | | |
| $[CuL^1]/[Cu][L^1]$ | 110 | 9.17(1) | 652 | 101 |
| $[Cu_2L^1H_{-2}][H]^2/[Cu]^2[L^1]$ | 21–2 | 1.451(6) | 652 | 202 |
| $[Cu_2L^1H_{-3}][H]^3/[Cu]^2[L^1]$ | 21–3 | −6.859(9) | | |
| $[Cu_2L^1H_{-4}][H]^4/[Cu]^2[L^1]$ | 21–4 | −16.45(1) | | |
| $[Cu_2L^1{}_2H_{-2}][H]^2/[Cu]^2[L^1]^2$ | 22–2 | 7.612(8) | 616 | 150 |
| $[CuL^1H_{-2}][H]^2/[Cu][L^1]$ | 11–2 | −5.860(5) | 526 | 134 |
| $[CuL^2]/[Cu][L^2]$ | 110 | 11.46(3) | 634 | 55 |
| $[Cu_2L^2H_{-2}][H]^2/[Cu]^2[L^2]$ | 21–2 | 4.268(9) | 634 | 110 |
| $[Cu_2L^2H_{-3}][H]^3$ /$[Cu]^2 2[L^2]$ | 21–3 | −4.45(1) | | |
| $[Cu_2L^2H_{-4}][H]^4/[Cu]^2[L^2]$ | 21–4 | −14.88(1) | | |
| $[Cu_3L^2{}_2H_{-4}][H]^4/[Cu]^3[L^2]^2$ | 32–4 | 4.50(3) | | |
| $[Cu_4L^2{}_3H_{-6}][H]^6/[Cu]^4[L^2]^3$ | 43–6 | 3.21(4) | | |
| $[CuL^2H_{-2}][H]^2/[Cu][L^2]$ | 11–2 | −3.69(1) | 537 | 67 |
| $[NiL^1H_{-2}][H]^2/[Ni][L^1]$ | 11–2 | −10.17(3) | 415 | 142 |

[a] Charges are omitted for clarity. [b] The standard deviation is given in parentheses.

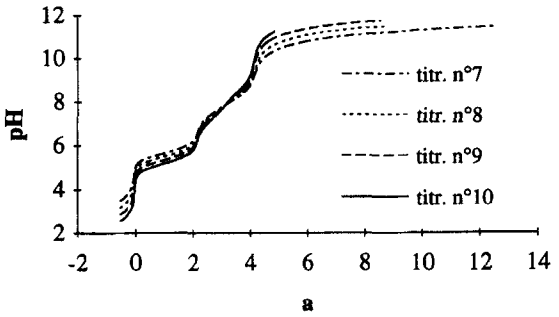


**Figure 2** M/L = 1/1 titrations curves of $Cu^{2+}$ and $L^1$. The titration number (titr.n°) is taken from Table I.

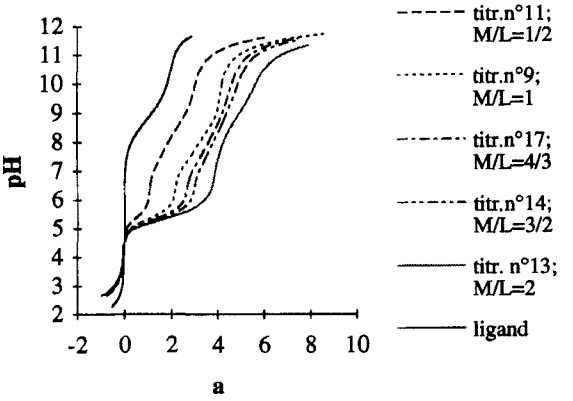


**Figure 3** Titrations curves of $Cu^{2+}$ and $L^1$; varying M/L ratio. The titration number (titr.n°) is taken from Table I.



According to Griesser, $Cu^{2+}$ and $L^1$ form CuL and $Cu_2LH_{-2}$ in this first buffer region.[3] Lloret suggests the sole formation of $Cu_2LH_{-2}$ for $L^2$.[5] Analysis of the potentiometric data of the first buffer region combined with a large number of spectra (visible region) taken during these titrations, led to the conclusion that both $L^1$ and $L^2$ form CuL and $Cu_2LH_{-2}$ complexes in the first buffer region of all potentiometric titrations in Table I. Analysis of the potentiometric data of $Cu^{2+}$ and $L^1$ is summarised in Table III. Here, both models (model 1: $Cu_2LH_{-2}$; model 2: CuL + $Cu_2LH_{-2}$) are evaluated using the titrations of $Cu^{2+}$ and $L^1$ or $L^2$ listed in Table I. Table III also includes the number of titration points used for minimisation and the $\sigma$ value (SUPERQUAD) of each of the titration curves. Finally, the model is evaluated by the $\sigma$ value and the standard deviation of the log$\beta$ values of a minimisation using all titrations at once. Table III clearly shows a significant improvement of all statistical parameters when the CuL complex is added to the system. In conclusion, both $L^1$ and $L^2$ form CuL and $Cu_2LH_{-2}$ complexes.

The structure of $Cu_2LH_{-2}$, determined by X-ray analysis is shown diagramatically in Figure 5.[16] Spectrophotometric titrations lack evidence for more than one $Cu^{2+}$ chromophore in the complexes of the first buffer region; $Cu^{2+}$ coordination modes in both complexes must therefore be similar. This results in a structure for CuL as

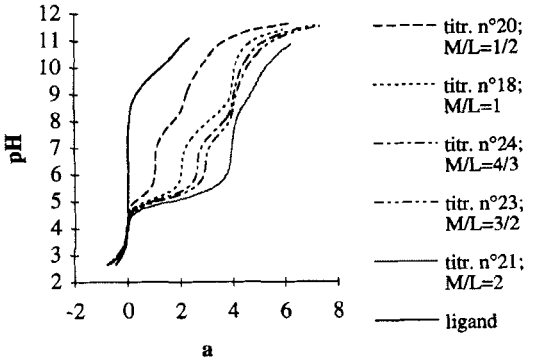


**Figure 4** Titrations curves of $Cu^{2+}$ and $L^2$; varying M/L ratio. The titration number (titr.n°) is taken from Table I.

**Table III** Statistical evaluation of two possible $Cu^{2+}$ complexation models with $L^1$ and $L^2$. Model 1: only $Cu_2L_2H_{-2}$ is formed in the first buffer region. Model 2: both CuL and $Cu_2L_2H_{-2}$ are formed.

| $Cu^{2+} + L^1$ | | | | $Cu^{2+} + L^2$ | | | |
|---|---|---|---|---|---|---|---|
| titr.n° [a] | #pts[b] | model 1 $\sigma$[c] | model 2 $\sigma$[c] | titr.n° [a] | #pts[b] | model 1 $\sigma$[c] | model 2 $\sigma$[c] |
| 7 | 11 | 1.4 | 1.3 | 18 | 8 | 6.8 | 3.1 |
| 8 | 12 | 2.6 | 2.3 | 19 | 11 | 9.9 | 3.0 |
| 9 | 15 | 6.8 | 2.5 | 20 | 10 | 2.4 | 6.0 |
| 10 | 12 | 7.6 | 4.4 | 21 | 15 | 10.0 | 4.3 |
| 11 | 16 | 8.8 | 3.1 | | | | |
| 12 | 23 | 13.4 | 2.6 | | | | |
| 13 | 14 | 10.1 | 4.0 | | | | |
| total | 103 | 7.4 | 3.1 | | 5.6 | 8.4 | 3.8 |
| $\log\beta CuL$[d] | | | 9.17(1) | $\log\beta CuL$[d] | | | 11.46(3) |
| $\log\beta Cu_2L_2H_{-2}$[d] | | 1.55(2)[e] | 1.451(6) | $\log\beta Cu_2L_2H_{-2}$[d] | | 4.35(2) | 4.268(9) |

[a] Number of titration (cf. table I). [b] Total number of experimental data points used in the refinement. [c] As calculated by SUPERQUAD, $\sigma = \Sigma_{i=1}^{z} w_i(E_i^{calc} - E_i^{obs})^2/(Z - m))^{0.5}$ where m is the number of parameters to be refined and Z is the total number of titration points. [d] I = 0.1 mol $dm^{-3}$, 25°C. [e] The standard deviation is given in parentheses.

depicted in Figure 6. Stability constants, molar absorptivities and $\lambda_{max}$-values for these complexes are given in Table II.

### *$Cu^{2+}$ complexes; second buffer region*

The final complex formed in alkaline conditions (pH > 8), $CuLH_{-2}$, is also similar for both ligands. These complexes have $\lambda_{max}$-values of 526 nm ($L^1$) and 537 nm ($L^2$) and $\varepsilon_{max}$-values of 134 $M^{-1}$ $cm^{-1}$ ($L^1$) and 67 $M^{-1}$ $cm^{-1}$($L^2$).

Stability constants for these complexes were derived with 110 ($L^1$) or 35 ($L^2$) titration points from 4 or 2 potentiometric titrations and the complete set of complexes in the second buffer region. The stability constants are given in Table II.

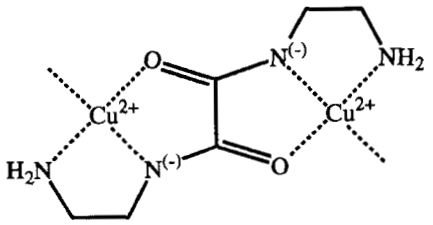


**Figure 5** Structural representation of $Cu_2L^1H_{-2}$ (counterions omitted).

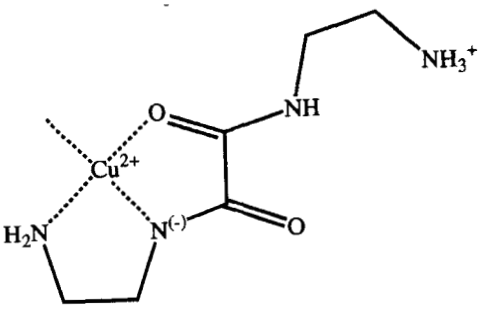


**Figure 6** Structural representation of $CuL^1$ (counterions omitted).



According to Lloret the second buffer region of $L^2$ is maintained by three complexes, $Cu_3L_2H_{-4}$, $Cu_4L_3H_{-6}$ and $CuLH_{-2}$. Analysis of both our potentiometric and spectrophotometric data was in accord with this proposal. Figure 7 shows the spectra taken in $L^2$ titration curve n° 29 (Table I). All values in bold are the a values reached in the titration at the moment the spectrum was recorded. We would like to focus on the appearance of an isosbestic point at 750 nm between a = 2 and 3. In this region, according to Lloret, only two complexes are present in solution,

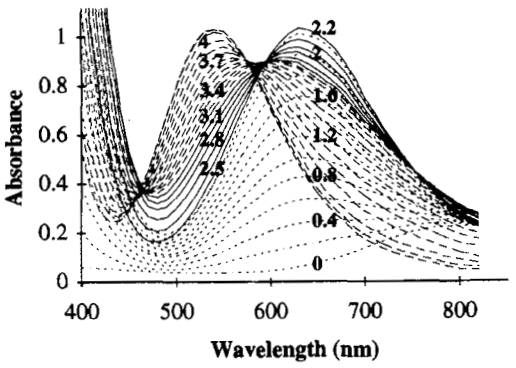


**Figure 7** Spectra (visible region) taken during titration n° 29. All numbers in bold correspond to the a-value in the titration.

$Cu_2LH_{-2}$ and $Cu_3L_2H_{-4}$. Therefore the increase in absorbance in the 800 nm region of the spectra is due to the formation of $Cu_3L_2H_{-4}$.

According to Griesser the second buffer region of the titrations of $Cu^{2+}$ and $L^1$ with metal:ligand ratios up to 1:1 is formed by two major complexes, $CuLH_{-1}$ and $CuLH_{-2}$.[3] In order to re-evaluate Griesser's proposal we carried out a series of 1:1 titrations over a large range of initial concentrations of metal ion and ligand. These titrations are shown in Figure 2. Starting from the stability constants given by Griesser, we simulated these titration curves. The resulting curves are shown in Figure 8. It is clear that with Griesser's model it is impossible to simulate the changing slope in the second buffer region. If the $CuLH_{-1}$ complex is replaced by its dimer $Cu_2L_2H_{-2}$ or by the analogue of Llorets $L^2$ proposal, $Cu_3L_2H_{-4}$, the changing slope can be simulated. However, for $Cu^{2+}$ complexation by $L^1$ the $Cu_3L_2H_{-4}$ species is not formed. This is demonstrated in Figure 9, which shows the experimental titration curve of $Cu^{2+}$ and $L^1$ at a 3:2 ratio together with two different simulations. The stability constants needed in these simulations are obtained from SUPERQUAD, using the titration points of all 1:1 titrations starting from two different sets of complexes. The first set contains CuL, $Cu_2LH_{-2}$, $Cu_2L_2H_{-2}$ and $CuLH_{-2}$. The second contains CuL, $Cu_2LH_{-2}$, $Cu_3L_2H_{-4}$, $Cu_4L_3H_{-6}$ and $CuLH_{-2}$ (the analogue for $L^1$ of Llorets proposal for $Cu^{2+}$ and $L^2$). In both sets of complexes the hydroxo complexes $Cu_2LH_{-3}$ and $Cu_2LH_{-4}$ were also included. These complexes will be discussed later. Obviously the first proposal results in a better fit; therefore $L^1$ and $L^2$ coordinate to $Cu^{2+}$ differently. Introduction of the alternative polynuclear complex $Cu_2L_2H_{-2}$ resulted in even better fits of the 1:1 titrations and the 4:3 titrations of $Cu^{2+}$ and $L^1$.

The formation of the $Cu_2L_2H_{-2}$ dimer is the prime reason why the slope of the buffer region depends on the concentration of the reagents. This is elucidated by plotting the relative maximum concentration ( = the maximum number of millimoles complex/total number of millimoles $Cu^{2+}$) of each of the complexes in the $Cu^{2+}$ + $L^1$ system for titration n° 7, 8, 9 and 10. This relative maximum concentration is clearly only influenced by the total concentration of $Cu^{2+}$ in the case of the polynuclear $Cu_2L_2H_{-2}$ complex (Figure 10). We used this enhanced formation of $Cu_2L_2H_{-2}$ to isolate this complex in the second buffer region. By extrapolating the relative concentration *versus* total $Cu^{2+}$ concentration curve to

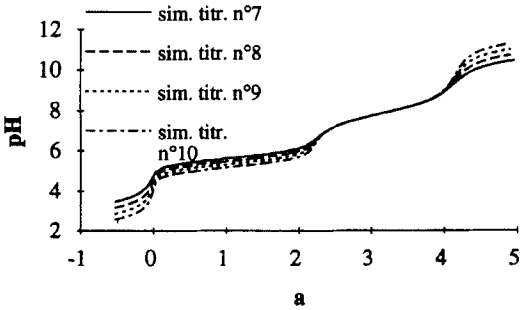


**Figure 8** Simulation of titrations n° 7 and n° 8, for the complex model $CuL^1$, $Cu_2L^1H_{-2}$, $CuL^1H_{-1}$, $CuL^1H_{-2}$.

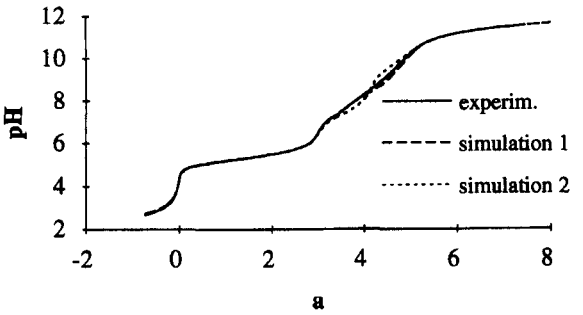


**Figure 9** Simulations of titration n° 15 (M/L = 3/2). Simulation 1 used complex model $CuL^1$, $Cu_2L^1H_{-2}$, $Cu_2L^1{}_2H_{-2}$, $CuL^1H_{-2}$, $Cu_2L^1H_{-3}$, $Cu_2L^1H_{-3}$, $Cu_2L^1H_{-4}$. Simulation 2 used complex model $CuL^1$, $Cu_2L^1H_{-2}$, $Cu_3L^1{}_2H_{-4}$, $Cu_4L^1{}_3H_{-6}$, $CuL^1H_{-2}$, $Cu_2L^1H_{-3}$, $Cu_2L^1H_{-4}$.

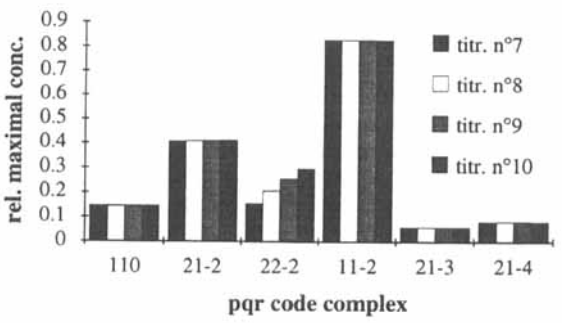


**Figure 10** Dependence of the $Cu^{2+}$ concentration of the relative maximal concentration of all complexes in titrations n° 7 to n° 10. Relative maximum concentration is maximum number of millimoles complex / total number of millimoles $Cu^{2+}$; pqr code corresponds to the $Cu_pL_qH_r$ complex.

obtain 100% formation of $Cu_2L_2H_{-2}$, we were able to calculate the appropriate concentrations for $Cu^{2+}$ and $L^1$ to guarantee the exclusive formation of this complex. However, under these optimum conditions (0.09 mol $dm^{-3}$ $Cu^{2+}$ and $L^1$, at pH = 8.0), the solubility of $Cu_2L_2H_{-2}$ is exceeded. The saturated solution was used to record an electronic spectrum (in solution) and the precipitate was subjected to an IR study.

In all minimisations we included the stability constants of the hydroxo complexes, $Cu_2LH_{-3}$ and $Cu_2LH_{-4}$, formed by substitution of the water sites of the $Cu^{2+}$ centres of $Cu_2LH_{-2}$ by hydroxo groups. These complexes appear mainly in titrations in which the metal: ligand molar ratio is 2:1. We checked the influence of $Cu_2L_2H_{-2}$ ($L^1$) and $Cu_3L_2H_{-4}$ and $Cu_4L_3H_{-6}$ ($L^2$) in these 2:1 titrations but these complexes do not appear in titrations at this Cu:L ratio. Furthermore, the influence of $Cu_2LH_{-3}$ and $Cu_2LH_{-4}$ proved to be minimal (to non existing) in the 1:1 titrations but not negligible in the 3:2 and 4:3 titrations.

### *$Cu_2L_2H_{-2}$; possibilities*

The $Cu_2L_2H_{-2}$ complex can be thought of as being assembled from previously formed complexes and ligand species in two ways. First, a combination of two CuL species is possible; a substitution of the coordinated water molecule of the first CuL entity by the ammonium group of the second one and *vice versa*, accompanied by the simultaneous deprotonation of these ammonium groups, results in the formation of $Cu_2LH_{-2}$. In that case, $Cu_2L_2H_{-2}$ can be described as in Figure 11. Another possibility involves reaction of excess $LH_2$ and $Cu_2L_2H_{-2}$. Again, this reaction involves deprotonation of two ammonium groups and results in an increase of one nitrogen donor per $Cu^{2+}$ centre in the complex. This change in the coordination sphere of $Cu^{2+}$ is clearly shown by comparing the $\lambda_{max}$-value of the $L^1$ complexes $Cu_2LH_{-2}$ ($\lambda_{max}$ = 652 nm) and $Cu_2L_2H_{-2}$ ($\lambda_{max}$ = 616 nm) (Table II).

### *$Cu_2L_2H_{-2}$; IR spectrum*

The proposed structure as given in Figure 11 is confirmed by the infrared spectrum of the solid compound isolated from the solution. According to the proposed ring structure we should observe the coordinated $NH_2$ group, the *N*-coordinated tertiary amide function and the *O*-coordinated *cis* secondary amide function, as typical groups. The 3303 $cm^{-1}$ ($\nu_{as}NH_2$), 3164 $cm^{-1}$ ($\nu_sNH_2$), 1168 $cm^{-1}$ ($\rho NH_2$) and 680 $cm^{-1}$ ($\tau NH_2$) bands indicate the coordinated $NH_2$ group. The intense 1661 $cm^{-1}$ ($\nu C = O$) and weak 1517 $cm^{-1}$ ($\nu CN$) are proof of the *N*-coordinated tertiary amide function. The 3258 $cm^{-1}$ ($\nu NH$), 1591 $cm^{-1}$ ($\nu C = O$), the broad 1410 $cm^{-1}$ ($\delta NH$) and 1315 $cm^{-1}$($\nu CN$) bands are typical of *cis* secondary *O*-coordinated amide functions. The absence in the infrared spectra of the typical intense amide II (1550 $cm^{-1}$) and amide III bands (1250 $cm^{-1}$) for *trans* secondary amide functions is a further confirmation of the structure as proposed in Figure 11.

### *$Ni^{2+}$ complexes*

Contrary to the complexation of $Cu^{2+}$ and $L^1$, complexation of $Ni^{2+}$ by $L^1$ occurs in a single buffer region. Our complex model is obtained mainly by analysis of the formation curves using equations (*2*) and (*3*) for the titration points of all 1:1

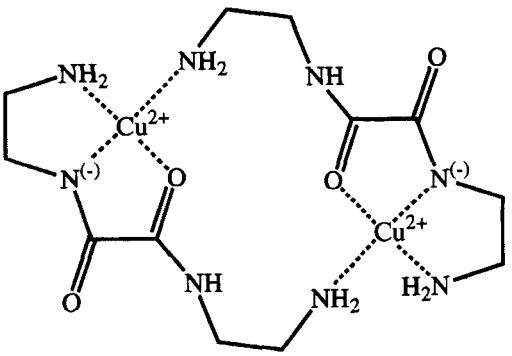


**Figure 11** Structural representation of $Cu_2L^1{}_2H_{-2}$ (counterions omitted).

titrations of $Ni^{2+}$ and $L^1$ (Table I). Formation plots ñ *versus* $pLH_x$, describing the formation of only one single mononuclear complex ($MLH_x$) have a fixed slope, which is independent of the stability of the complex.[17] The formation curve of titration n° 31, in which every point was measured after no more than 5 minutes of equilibration time, differs significantly from this theoretical plot for the formation of a single 1:1 complex. The second formation plot (titration n° 38) used the titration points of a 1:1 titration with more than 1 hour of equilibration time. This formation curve approaches the theoretical 'single 1:1 complex' curve. Finally, the formation curve for the out-of-cell titration n° 39 (equilibration time of 3 days) clearly shows the formation of only one 1:1 complex (Figure 12). The end inflection point of all titrations agree with the maximum formation of $NiLH_{-2}$.

Electronic spectra support this conclusion by showing the growth of only one chromophore until a = 4 (Ni:L = 1:1) is reached. $NiLH_{-2}$ clearly is square planar with a $\lambda_{max}$-value of 415 nm and $\varepsilon_{max}$ = 142 $M^{-1}$ (Table II). The titration curves of $Ni^{2+}$ + $L^2$ could not be used to calculate stability constants for this system because complexation was either too slow or was too weak to avoid competition with ligand hydrolysis and $Ni(OH)_2$ formation.

The stability constants of the copper complexes are not easily interpreted due to the uncertainty of the deprotonation constants of the amide groups of these oxamide ligands. Since all complexes possess deprotonated amide groups, a true interpretation of the constants necessitates at least a very good estimation of the deprotonation constants. Secondly, the logβ value of the ML complex cannot be used to derive the $pK_a$ values for complex amide deprotonation because in order to obtain these constants the ML entity of the equilibrium $[ML] \leftrightharpoons [MLH_{-1}]^{-1} + H^+$ should not contain a deprotonated amide groups.

Because of the near identity of the amide groups in both $L^1$ and $L^2$, it is possible to compare the stability constants of $MLH_{-2}$ for both ligands. The logβ value of the $L^2$ complex possessing a 6, 5, 6 chelate ring structure is 2.17 logβ units higher than the logβ value of the 5, 5, 5 ring complex of $L^1$. This increase in stability of the 6, 5, 6 ring sequence complexes is also the main reason why the intermediate polynuclear complexes of $L^1$ and $L^2$ have a different composition. The $Cu_2L_2H_{-2}$ complex of $L^1$ possesses two adjacent five-membered rings and the ligand is in its *trans* configuration. The $Cu_3L_2H_{-4}$ complex of $L^2$ however possesses the 6, 5, 6,

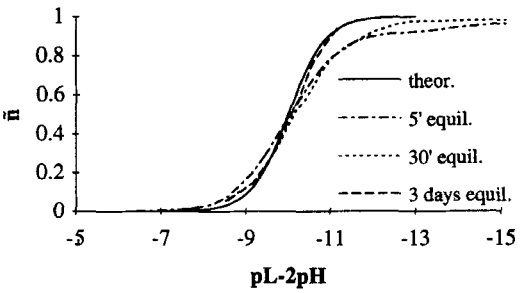


**Figure 12** Formation curves for the $Ni^{2+}$ + $L^1$ titration curves n° 31, n° 38 and n° 39. The solid line corresponds to the theoretical formation curve for the formation of a single 1:1 complex in its own buffer region; 'equil' stands for 'equilibration time'.

chelate ring system in the $CuLH_{-2}$ complex, which suggests that the negative effect of *cis* orientation of the oxamide group is overcome by the positive effect of chelate ring structure.

$Ni^{2+}$ does not form complexes with $L^1$ in which the oxamide group is in a *trans* configuration. This is a consequence of the fact that, unlike $Cu^{2+}$, the $Ni^{2+}$ ion needs more than one amino group anchor to deprotonate and coordinate amide groups.[1] For $L^1$ the combination of both terminal amino groups acting as anchors, and the formation of consecutive 5, 5, 5 chelate ring sequence is the driving force for the formation of a single $NiLH_{-2}$ complex. We note that the smaller ligand $L^1$ is able to form a more stable $NiLH_{-2}$ complex than $L^2$, in spite of the possibility of ring alternation with the latter.

*Acknowledgements*

The authors which to thank Ing. W. Lippens for technical assistance. A grant from Het Eigen Onderzoeksfonds van de Universiteit Gent (01171091-OZF) is greatly appreciated.



*References*

1. H. Sigel and R.B. Martin, *Chem. Rev.*, **82**, 385 (1982).
2. H. Ojima and K. Nonoyama, *Coord. Chem. Rev.*, **92**, 58 (1988).
3. R. Griesser and S. Fallab, *Chimia*, **22**, 90 (1968).
4. F. Lloret, M. Julve, J. Faus, Y. Journaux, M. Philoche-Levisalles and Y. Jeannin, *Inorg. Chem.*, **28**, 3702 (1989).
5. F. Lloret, M. Julve, J. Faus, R. Ruiz, I. Castro, M. Mollar and M. Philoche-Levissalles, *Inorg. Chem.*, **31**, 784 (1992).
6. F. Lloret, M. Julve, J.A. Real, J. Faus, RT. Ruiz, M. Mollar, L Castro and C. Bois, *Inorg. Chem*, **31**, 2956 (1992).
7. F. Lloret, J. Sletten, R. Ruiz, M. Julve, J. Faus and M. Verdaguer, *Inorg. Chem.*, **31**, 778 (1992).
8. A. I. Vogel, *A Text-book of Quantitative Analysis* (Longmans and Green, New York, 1961), p. 959.
9. A. P. Arnold, S. A. Daignault and D.L. Rabenstein, *Anal. Chem.*, **57**, 1112 (1985).
10. G. Gran, *Analyst (London)*, **77**, 661 (1952).
11. A.E. Martell and R.M. Smith, *Critical Stability Contants* (Plenum Press, New York 1985), Vol. 5.
12. A. Sabatini, A. Vacca and P. Gans, *Coord. Chem. Rev.*, **120**, 398 (1992).
13. P. Gans, A. Sabatini and A. Vacca, *J. Chem. Soc., Dalton Trans.*, 1195 (1985).
14. Ting-Po I. and G.M. Nancollas, *Anal. Chem.*, **41**, 1940 (1972).
15. E. Leporati, *J. Coord. Chem.*, **33**, 179 (1994).
16. V.G. Albano, C. Castellari, A. G. Fabretti and A. Giusti, *Inorg. Chim. Acta*, **191**, 213 (1992).
17. F.J.C. Rossotti and N. Rosotti, *The Determination of Stability Contants* (McGraw-Hill Book Company, 1961), p. 40.